

1 **Chelating agents supported solar photo-Fenton and sunlight/H₂O₂ processes for**
2 **pharmaceuticals removal and resistant pathogens inactivation in tertiary treatment for urban**
3 **wastewater reuse.**

4

5 **Pellegrino La Manna^a, Marco De Carluccio^a, Patrizia Iannece^b, Giovanni Vigliotta^b, Antonio**
6 **Proto^c, Luigi Rizzo^{a*}**

7 *^a Water Science and Tecnology group (WaSTe), Department of Civil Engineering, University of*
8 *Salerno, Via Giovanni Paolo II 132, 84084 Fisciano (SA), Italy.*

9 *^b Department of Chemistry and Biology, University of Salerno, Via Giovanni Paolo II 132, 84084*
10 *Fisciano (SA), Italy*

11 *^c Environmental Chemistry Group (ECG), Department of Chemistry and Biology, University of*
12 *Salerno, Via Giovanni Paolo II 132, 84084 Fisciano (SA), Italy*

13

14 Pre-review version of the manuscript published in Journal of Hazardous Materials 452, 15 June
15 2023, 131235, <https://doi.org/10.1016/j.jhazmat.2023.131235>

16

17

18

19 * Corresponding Author, e-mail addresses: l.rizzo@unisa.it

20

21 **ABSTRACT**

22 In this work, Fe³⁺-iminodisuccinic acid (Fe:IDS) based solar photo Fenton (SPF) was investigated in
23 tertiary treatment of real urban wastewater and compared to Fe³⁺-ethylenediamine-N,N'-disuccinic
24 acid (Fe:EDDS) for the first time. Three pharmaceuticals (PCs) (sulfamethoxazole, carbamazepine
25 and trimethoprim) and four pathogens (*Escherichia coli*, somatic and F-plus coliphages, *Clostridium*
26 *perfringens*, consistently with the new EU regulation for wastewater reuse (2020/741)), were chosen
27 as target pollutants. The best operating conditions resulted: H₂O₂=50 mg L⁻¹; Fe=0.1 mM; Fe:L=1:1;
28 alkalinity=75 mg L⁻¹ for both Fe:Ligand (Fe:L) based SPF processes. SPF with Fe:EDDS was more
29 effective in PCs removal (80%, 10 kJ L⁻¹) than the SPF with Fe:IDS (58%). On the contrary, Fe:IDS
30 resulted more effective (4.3 log inactivation for *E. coli*) than Fe:EDDS (1.9 log) in pathogens
31 inactivation. Fe:L based SPF was subsequently coupled to sunlight/H₂O₂. Interestingly, while its
32 combination with Fe:EDDS based SPF slightly increased disinfectant efficacy (2.3 vs 1.9 log
33 inactivation for *E. coli*), the combination with Fe:IDS showed an opposite effect (3.4 vs 4.3 log
34 reduction). Such results, make the use of Fe:IDS an attractive option in SPF tertiary treatment for
35 urban wastewater reuse.

36

37 *Keywords:* advanced oxidation processes; contaminants of emerging concern; natural pH; photo-
38 Fenton like; viruses.

39

40 **ENVIRONMENTAL IMPLICATION STATEMENT**

41 Pharmaceuticals and pathogens are considered as hazardous chemical and biological pollutants and
42 are among the main environmental and health challenges in tertiary treatment of urban wastewater
43 for reuse. In particular, pharmaceuticals have been recently included in the new EU wastewater
44 reuse regulation as hazardous pollutants to take into account within the risk management plan.
45 Accordingly, in this work a sustainable solution for small wastewater treatment plants coupling
46 sunlight/H₂O₂ and solar photo Fenton (SPF) with a new chelating agent was compared to a
47 consolidated chelating agent to effectively remove such pollutants and operate SPF at neutral pH.
48

1. Introduction

Climate change, pollution, population growth and conflicts are among the main factors causing high water-stress across the globe (Wang et al., 2021). Preserving water quality and ensuring its availability is one of the most serious challenges for several countries in the world (Kummu et al., 2016, UN World Water Development Report 2020). Indeed, around four billion of people face severe water scarcity every day (Mekonnen et al., 2016). In particular, climate change is causing serious problems even in geographical areas only marginally or not affected by water scarcity until a few years ago. In this context, wastewater reuse represents an excellent strategy to overcome the water crisis (Scheierling et al., 2011; Villarín and Merel, 2020). At the same time, caution should be taken in applying this practice, since improper treatments can lead to dramatic consequences (Fatta-Kassinos et al., 2011). While in low-income countries, the main risk factor in the practice of wastewater reuse is the presence of pathogenic microorganisms, in high-income countries contaminants of emerging concern (CECs) must also be considered (Fatta-Kassinos and Costas, 2013; Pastorino and Ginebreda, 2021). CECs include active ingredients of pharmaceuticals (PCs), pesticides, personal care products etc., that although occurring at low concentrations (in the range ng L^{-1} - $\mu\text{g L}^{-1}$) in water and wastewater, can accumulate in the environment resulting in chronic toxic effects (Christou et al., 2017; Hossain and Roy, 2018). Moreover, among PCs, antibiotics are of additional concern because can trigger antibiotic resistance, which represents a serious threat to human health (Cacace et al., 2019). Unfortunately, commonly employed processes in urban wastewater treatment plants (WTPs) are scarcely efficient in the removal of CECs and the scientific community is committed in investigating possible solutions for an effective and sustainable tertiary treatment (Rizzo et al., 2019). Advanced oxidation processes (AOPs), relying upon the build-up of highly reactive oxygen species (ROS), are among the most investigated solutions for tertiary treatment of urban wastewater (Comninellis et al., 2008; Deng et al., 2015; Rizzo, 2022). Particularly, solar photo-Fenton (SPF) like process, implementing chelating agents to effectively operate the

74 process at neutral pH, it allows to overcome the limitation of the conventional process which is
75 effective at acidic pH and it has been attracting increasing interest as possible solution in small WTPs
76 (Prieto-Rodríguez et al., 2013; De la Obra et al., 2017; Fiorentino et al., 2019; Oller and Malato,
77 2021; Gualda-Alonso et al., 2022). Such an interest is expected to further increase in the next years
78 because the growing energy cost, water scarcity and sustainability policies are driving toward the
79 implementation of sustainable green solutions for wastewater treatment and reuse. The presence of
80 chelating agents in SPF like process delays the precipitation of iron at neutral pH, allowing an
81 effective degradation of the target pollutants (Clarizia et al., 2017). Polycarboxylic and
82 aminopolycarboxylic acids have been used as ligands for iron species (Baba et al., 2015; Prete et al.,
83 2021) and ethylenediamine-N,N'-disuccinic acid (EDDS) has been successfully investigated in the
84 degradation of CECs by SPF in secondary treated urban wastewater (Miralles-Cuevas et al., 2019;
85 Maniakova et al., 2020). However, chelating agent supported SPF has still some drawbacks: (i) EDDS
86 is quite expensive, making the process not yet competitive compared to conventional SPF at acidic
87 pH (Sánchez Pérez et al., 2020); (ii) while Fe:EDDS supported SPF can provide a higher removal of
88 CECs compared to sunlight/H₂O₂, it is less effective in bacteria inactivation (Maniakova et al.,
89 2021a).

90 Iminodisuccinic acid (IDS), a biodegradable ligand (Schowanek et al., 1997; Cokesa et al., 2004), has
91 been recently investigated as a chelating agent in water treatment (Fiorentino et al., 2021; Faggiano
92 et al., 2022) and disinfection (Fiorentino et al., 2018), making the potential of Fe:IDS complex in
93 tertiary treatment of urban wastewater by SPF worthy of investigation.

94 To speed up the possible application of SPF at full scale, in particular as tertiary treatment in
95 wastewater reuse applications, tests under realistic conditions using real wastewater, different CECs
96 and microorganisms should be implemented (Rizzo et al., 2020). The regulation of CECs in
97 wastewater reuse has been widely debated (Rizzo et al., 2018; Deviller et al., 2020) before being
98 introduced into the European regulation (2020/741). Accordingly, the relevant stakeholders are asked
99 to take the occurrence of CECs into account, through a risk assessment plan, when authorizing reuse

100 of WTPs effluents. Moreover, the validation control, by including really stringent targets for
101 pathogens inactivation (namely, \log_{10} reductions ≥ 5.0 for *Escherichia coli*, ≥ 6.0 for different types
102 of coliphages and ≥ 4.0 for *Clostridium perfringens*), make the identification of effective and
103 sustainable tertiary treatment methods even increasingly challenging.

104 In this work, SPF process with Fe:IDS complex was investigated for the first time as tertiary treatment
105 of urban wastewater at natural pH and compared to SPF with a consolidated complex, namely
106 Fe:EDDS. Moreover, SPF was also compared to sunlight/H₂O₂ and to their combination through a
107 sequential treatment approach in the effort to maximize both PCs removal and pathogens inactivation.
108 Solar driven tests were carried at pilot scale in raceway pond reactors (RPRs), which are considered
109 a cheaper solution compared to compound parabolic collectors-based reactors (Carra et al., 2014).
110 The target PCs (sulfamethoxazole (SMX), trimethoprim (TMP) and carbamazepine (CBZ)) were
111 selected as a result of a compromise among different factors: (i) their occurrence in urban wastewater
112 and refractoriness to conventional wastewater treatment, (ii) representativeness of relevant
113 pharmaceutical families/functions and (iii) relevance for crop uptake (Krzeminski et al., 2019;
114 Christou et al., 2019). Different concentrations of Fe, Fe:L ratios and alkalinity values were
115 investigated in terms of pharmaceuticals (PCs) removal. As the operating conditions were optimized,
116 the disinfection capacity was investigated on different pathogens including *E. coli*, as indicators of
117 pathogenic bacteria, coliphages as indicators of pathogenic viruses and *C. perfringens* as indicators
118 of protozoa, consistently with the approach used in the EU regulation on wastewater reuse.

119 **2. Materials and methods**

120 **2.1 Chemicals and reagents**

121 High-purity grade (>99%) SMX, CBZ and TMP were sourced from Sigma Aldrich. Catalase from
122 bovine liver, EDDS water solution (35%, w/v), Titanium (IV) Oxysulfate (99.99%), 1,10-
123 phenanthroline (99%), ammonium acetate (98%) and acetic acid (99%) were purchased by Sigma

124 Aldrich. An Arium Mini Deionizer (Sartorius) produced deionized water employed in the
 125 experiments. FeCl₃·7H₂O (98%) and H₂O₂ (35%, w/v) were purchased from Carlo Erba Reagents.
 126 Acetonitrile (ACN) (LC-MS grade), formic acid (FA) (LC-MS grade) and H₂O (LC-MS grade) were
 127 purchased from Honeywell. Nalidixic acid, Indoxyl-B-D-glucoside, Polymyxin B Sulfate, D-
 128 Cycloserine, Phenolphthalein Diphosphate Tetrasodium salt were purchased from VWR. Tryptone bile
 129 X-glucoronide (TBX) Agar, Nutrient Brooth, Kovacs Reactant, Agar, m-CP Agar, *E. coli* ATCC
 130 13706 and ATCC 15597 strains, Tryptone and Tryptone Soy Agar were purchased from Biolife.
 131 Ampicillin Sodium Salt (>99%), Magnesium Sulfate Heptahydrate (≥ 99.5%), Sodium Chloride
 132 (>99%), Sodium Dihydrogen Phosphate (≥ 99%), Potassium Phosphate dibasic (≥98%), EDDS and
 133 Ammonia solution (28%) were purchased by Sigma Aldrich. Anaerobic jars (2.5 L volume) were
 134 purchased from Oxoid. IDS was purchased by Glentham Life Sciences.

135

136 2.2 Wastewater characteristics

137 Secondary wastewater samples were collected from a WTP located in the province of Salerno, Italy
 138 (650000 equivalents inhabitants) implementing a conventional activated sludge process as biological
 139 treatment. Chemical and microbiological characteristics of the collected secondary effluent are
 140 reported in Table 1.

141

142 Table 1. Chemical and Microbiological Characteristics of the secondary wastewater.

Parameter	Mean value
pH	7.2 ± 0.1
COD (mg L ⁻¹) ²	11 ± 2
BOD ₅ (mg L ⁻¹) ²	2 ± 1
Alkalinity (HCO ₃ ⁻) (mg L ⁻¹)	330 ± 10
Total Suspended Solids (mg L ⁻¹)	6 ± 1

Turbidity (NTU)	0.47 ± 0.05
Total Nitrogen (mg L⁻¹)	3 ± 0.2
Chlorides (mg L⁻¹)	126 ± 11
NO₃⁻-N (mg L⁻¹)	2 ± 0.2
NO₂⁻-N (mg L⁻¹)	nd
<i>E. coli</i> (CFU¹ 100 mL⁻¹)	(2.9 ± 0.2) x 10 ⁴
Coliphages (PFU³ 100 mL⁻¹)	(1.1 ± 0.1) x 10 ⁴
<i>C. perfringens</i> (CFU¹ 100 mL⁻¹)	(1.0 ± 0.1) x 10 ³

143 ¹CFU: colony forming units. ² COD and BOD₅ values in Table 1 are lower of those generally reported in literature,
144 because of the low organic load factor of the WTP. ³PFU: plaques forming units.

145

146 **2.3 Solar driven tests in RPR**

147 **2.3.1 Experimental set-up**

148 Experiments in RPR (90 cm x 45 cm, 15 cm liquid depth and a working volume of 15 L) were carried
149 out under natural solar irradiation at University of Salerno, Fisciano Campus, Southern Italy (40°76'N
150 and 14°79'W), in sunny days during summer, from 11:00 to 14:00 local time, in order to exploit an
151 approximatively constant solar radiance in the range 40-60 W m⁻². Irradiances varying in this range
152 are not a limiting factor for SPF process in RPR (Cabrera-Reina et al., 2021). The RPR is equipped
153 with a paddle wheel connected to an engine (with variable frequency, in the experiments it was set to
154 18 rpm) to facilitate the mixing of the chemical compounds (Fe complex, H₂O₂) in the aqueous
155 solution. The total exposure for each experiment was 180 min. Irradiance spectra were measured in
156 the range 280-400 nm by a radiometer (BLACK-Comet Stellar Net UV-VIS, StellarNet, Tampa, FL,
157 USA) mounted on a horizontal platform. In PCs degradation tests, SMX, CBZ and TMP were spiked
158 in the wastewater samples at an initial concentration of 0.2 mg L⁻¹ each one (7.5 mL of stock solution).
159 In disinfection experiments the effect on the indigenous bacteria population was evaluated. The

160 results were plotted as a function of the accumulated UV energy per unit of treated volume (Q_{UV} , kJ
161 L^{-1}) (Malato et al., 2003):

$$162 \quad Q_{UV,n} = Q_{UV,n-1} + \Delta t_n \cdot \overline{UV}_{G,n} \cdot \frac{A_r}{V_t} \quad (\text{Eq. 1})$$

163 In the above equation, V_t is the total volume of water (L). Q_{UV} represents the UV energy per treated
164 volume between samples n and $n-1$, $\overline{UV}_{G,n}$ ($W m^{-2}$) represents the average UV radiation measured,
165 Δt_n and A_r are the experimental time between samples and the illuminated area (m^2), respectively.

166 Different Iron:Ligand (Fe:L) ratios were investigated while an initial concentration of 50 mg L^{-1} (1.47
167 mM) of H_2O_2 was used, according to previous works (De La Cruz et al., 2013; Fiorentino et al.,
168 2019). Sunlight/ H_2O_2 experiments were performed with the same concentration of H_2O_2 . Sequential
169 treatment tests combining sunlight/ H_2O_2 and SPF processes were performed starting with the
170 sunlight/ H_2O_2 process for 60 min and continuing with SPF for a total time of 180 min.

171 After adding the treated secondary wastewater sample in the RPR, H_2O_2 was added in one step and
172 the aqueous solution was stirred for 2 min at 36 rpm. Subsequently, the iron complex (Fe:IDS or
173 Fe:EDDS) was added and recirculated. In the PCs degradation tests, the contaminants (TMP, CBZ,
174 SMX; 0.2 mg L^{-1}) were added at the beginning before adding the oxidant (H_2O_2). The resulting
175 solution was mixed for 2 min before removing the cover from the RPR. Water temperature was
176 monitored during the experiments and was always under $40 \text{ }^\circ\text{C}$ (30-38 $^\circ\text{C}$), therefore no significant
177 temperature effect on bacteria inactivation was expected (O'Dowd and Pillai, 2020). For PCs
178 removal, sampling times were 15, 30, 45, 60, 90, 120 and 180 min. For bacteria inactivation, sampling
179 times were 15, 30, 45, 60, 75, 90, 105, 120, 150 and 180 min.

180

181 **2.3.2 Preparation of Fe:L complexes and PCs stock solution**

182 Fe:L complexes were prepared by dissolving the appropriate amount of $FeCl_3 \cdot 7H_2O$ in deionized
183 water and adding the desired amount of freshly prepared chelating agent solution (EDDS and IDS,

184 respectively) and the mixture was vigorously stirred for 10 min under dark, to avoid the instability of
185 the complex. In the case of Fe:EDDS complex, one drop of H₂SO₄ solution (95%) was also added to
186 improve the solubility of the complex. PCs stock solution was prepared dissolving PCs (16 mg each
187 one) in 40 mL aqueous solution (90/10 H₂O/EtOH).

188

189 **2.3.3 Alkalinity effect**

190 To evaluate the effect of alkalinity on SPF tests, the spontaneous alkalinity value (330 mg L⁻¹) was
191 adjusted to 75, 150 and 600 mg L⁻¹, respectively. Specifically, 2.8 mL of H₂SO₄ concentrated solution
192 (95%) were added to 30 L wastewater to get a final alkalinity of 75 mg L⁻¹ (pH = 6.8) and 1.5 mL in
193 30 L for a final alkalinity of 150 mg L⁻¹ (pH = 7.0). The final samples were purged overnight by an
194 air bubbler to remove CO₂ formed following the acidification. To increase the alkalinity to 600 mg
195 L⁻¹, NaHCO₃ (99%) was added to the sample (final pH = 7.5).

196

197 **2.4 Analytical measurements**

198 PCs concentration was measured by Ultra-Performance Liquid Chromatography (Ultimate™ 3000
199 Basic Automated System, ThermoScientific) equipped with an UV-DAD detector, column thermostat
200 and an automated sample injector (loop volume: 100 µL). PCs separation was achieved on a reversed-
201 phase Luna C18 column (150x4.6 mm, 5 µm, 100 Å), by using gradient elution with 0.1% formic
202 acid in water (v/v, eluent A) and 0.1% formic acid in acetonitrile (v/v, eluent B) at a flow rate of 1
203 mL min⁻¹. The gradients were as follows: 0-10 min from 2% to 85% B; 10-12 min to 85% B; 12-13
204 min from 85% to 2% B (initial conditions); 2 min to 2% B (reconditioning). The column temperature
205 was set at 40°C. The injection volume was 10 µL. Wavelength of maximum absorbance for SMX,
206 CBZ and TMP was 270 nm. Retention times for TMP, SMX and CBZ were 6.54 min, 8.67 min and
207 9.43 min, respectively.

208 Aqueous samples for the analytic measurements (10 mL) were collected using a 15 mL plastic syringe
209 (10 mL) at fixed time intervals, filtered through 0.45 μm PTFE filter (Merck Millipore), if PCs
210 determination was needed; for bacteria enumeration, this last operation was ruled out.
211 Spectrophotometric determination of iron and H_2O_2 concentration was performed by a UV/Vis
212 Lambda-25 spectrophotometer (Perkin Elmer). H_2O_2 concentration was determined according to DIN
213 38 402 H15 method: measurement at 410 nm wavelength of the solution obtained adding 0.3 mL of
214 titanium (IV) oxysulfate to 3 mL sample previously filtered (0.45 μm PTFE filter) was carried out.
215 Dissolved Fe concentration was measured according to ISO 6332:1988 method, by analyzing the
216 absorbance at 510 nm wavelength of the solution obtained by adding 1,10-phenantroline to 10 mL of
217 previously filtered (0.45 μm PTFE filter) sample and subsequently acidified.
218 Chemical Oxygen Demand (COD), Alkalinity, Total Nitrogen, Nitrites and Nitrates concentrations
219 were determined spectrophotometrically using the appropriate test kit (HACH). BOD_5 was measured
220 by manometric method pouring freshly collected secondary wastewater (432 mL) in Oxitop[®]
221 respirometer bottles (Xylem, USA). pH was measured by a pH meter (HANNA Edge[®]), the
222 instrument being calibrated before its use. Turbidity measurements were obtained by a HACH 2100N
223 Turbidimeter.

224

225 **2.5 Microbiological analysis**

226 Samples (60 mL) taken during SPF and sunlight/ H_2O_2 experiments were mixed with 1.2 mL of bovine
227 liver catalase solution (0.2 g L^{-1} stock solution in deionized water) to quench H_2O_2 residual
228 concentration before microbial analysis. Subsequently, enumeration of bacteria was performed by
229 standard plate counting method (Double Agar Layer, lysis plaque method for somatic coliphages)
230 and filtration membrane method (all the experiments were carried out in triplicate) using the
231 following media: Triptone Bile X-Glucuronide and Triptone Soy Agar for *E. coli*; m-CP Agar (mixed
232 with polymyxin B sulfate, D-cycloserin and indoxyl- β -D glucoside) for *C. perfringens*; Triptone Agar

233 (mixed with nalidixic acid for somatic coliphages; with ampicillin sodium salt and streptomycin for
234 F-plus coliphages) and inseminated with a solution of *E. coli* ATCC 13706 strain or *E. coli* ATCC
235 15597 for coliphages (dual layer agar technique). Plates were incubated at 37°C for 24 h and at 44°C
236 for 24 h (in anaerobic jar) for *E. coli* and *C. perfringens*, respectively. For coliphages, an aliquot of a
237 18 h cultured host selected bacterial strain was mixed with overlay agar (pre-heated at 45°C).

238 **3. Results and discussion**

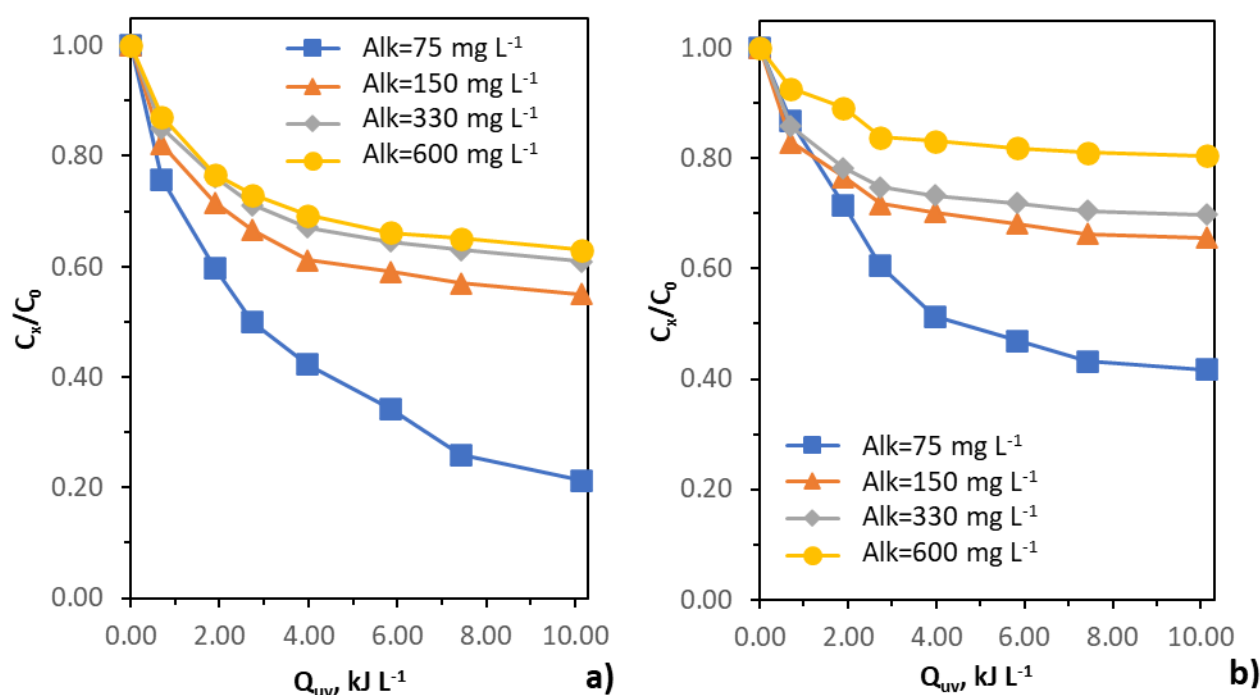
239 ***3.1 Effect of operating conditions on SPF performances***

240 The operating conditions of the SPF process with the two catalysts under study (Fe:EDDS and
241 Fe:IDS) were optimized by evaluating: (i) the effect of wastewater alkalinity on PCs removal and *E.*
242 *coli* inactivation; (ii) the effect of Fe concentration and Fe:L ratio on PCs removal. In all trials the
243 initial H₂O₂ dosage was set at 50 mg L⁻¹.

244 ***3.1.1 Effect of wastewater alkalinity on PCs removal and E. coli inactivation***

245 Although the negative effect of alkalinity on the AOPs efficiency is well known, as carbonates act as
246 hydroxyl radical (HO[•]) scavengers (Pignatello et al., 2006; Papoutsakis et al., 2015) and are able to
247 lead to the break-up of iron chelates (Miralles-Cuevas et al., 2014), in this work such effect was
248 evaluated systematically to verify to which extent alkalinity comparatively affects the two complexes.
249 The higher the alkalinity, the lower SPF process efficiency in terms of PCs degradation (Figure 1a
250 and 1b). Interestingly, the effect of the alkalinity is more pronounced for EDDS than IDS. As the
251 alkalinity increased from 75 mg L⁻¹ to 150 mg L⁻¹, a drastic decrease in the mean value of PCs removal
252 efficiency (from 78% to 50%) was observed for the Fe:EDDS supported process (Figure 1a), while a
253 lower decrease was observed for Fe:IDS (from 58% to 38%) (Figure 1b). Taking into account that
254 radical species attack in a non-selective manner all the organic compounds (Deng and Zhao, 2015),
255 the most probable explanation for the differences detected between these two complexes is given by

256 the inferior capability of generating radical species by Fe:IDS in presence of sunlight and H₂O₂. The
 257 higher capability of generating HO[•] by Fe:EDDS was partially thwarted by the preferential attack of
 258 the produced radicals to the more abundant ligand and carbonates rather than PCs (only 0.2 mg L⁻¹).
 259 Indeed, the reaction of HO[•] with carbonates (CO₃²⁻/HCO₃⁻) leads to the formation of carbonate
 260 radicals (HCO₃[•]/CO₃^{•-}) that are 3 times less reactive than HO[•] worsening the side effects of radical
 261 scavenging phenomenon (Ji et al., 2015; Lofrano et al., 2021). In parallel, the effect of alkalinity on
 262 wastewater disinfection was evaluated using *E. coli* as target bacteria, being among the most used
 263 indicators for wastewater disinfection and reuse and recently included in the first European regulation
 264 on wastewater reuse for agricultural applications (EU 2020/741). Consistently with the results for
 265 PCs removal, the optimal operative conditions were proved to be 75 mg L⁻¹ in terms of alkalinity.
 266 (Figure S2).



267
 268 **Figure 1.** Effect of wastewater alkalinity (from 75 mg L⁻¹ to 600 mg L⁻¹) on PCs degradation by SPF process with
 269 Fe:EDDS (a) and Fe:IDS (b). Total time=180 min, H₂O₂=1.47 mM, Fe:L=0.1 mM:0.1 mM.

270 **3.1.2 Effect of Fe concentration and Fe:L ratio on PCs removal**

271 Once the optimal alkalinity condition for PCs removal was identified, the subsequent experiments,
272 aimed at optimizing the catalyst dosage (Fe concentration and Fe:L ratio), were carried out under the
273 same alkalinity conditions (75 mg L^{-1}). Indeed, while H_2O_2 dose in SPF like process for tertiary
274 treatment of urban wastewater is well known from the literature (De La Cruz et al., 2013; Fiorentino
275 et al., 2019), iron initial dose and Fe:L ratio can change in a narrow range, depending on wastewater
276 characteristics, and significantly affecting process efficiency. Accordingly, three iron doses and two
277 Fe:L ratios were investigated. The best operative condition resulted to be 0.1 mM Fe, 0.1 mM for
278 both chelating agents (Table 2). SPF with Fe:EDDS (0.1 mM, molar ratio Fe:EDDS = 1:1, $\text{H}_2\text{O}_2 =$
279 50 mg L^{-1}) was effective in the degradation of the target PCs, in particular in the early 60 min ($Q_{\text{uv}} =$
280 4.14 kJ L^{-1}) of the experiment where the average removal was as high as 61% (Figure S1).
281 Consistently with these results, the H_2O_2 consumption rate was fast (Figure S1) and relevant in the
282 early 60 min (77%). SMX showed to be the most degradable contaminant (82%), followed by CBZ
283 (77%) and TMP (76%) (Table 2). Subsequently, the removal rate slowed down, and from 120 min
284 ($Q_{\text{uv}} = 7.4 \text{ kJ L}^{-1}$) until the end of the test, PCs residual concentrations did not show a remarkable
285 decrease. These results are consistent with previous works available in literature under comparable
286 operating conditions (Maniakova et al., 2022a).

287 Noteworthy, an increase in Fe concentration (from 0.1 mM to 0.2 mM) or in the Fe:L ratio (from 1:1
288 to 1:1.5) did not positively affect the process, regardless of the ligand exploited. EDDS can be an
289 easy target for HO^\bullet (Wu et al., 2014), therefore the decreased efficiency of the process as the ligand
290 dose was increased can be due to a massive consumption of radicals, leading to unsatisfactory results
291 in terms of PCs removal. A similar result was also observed for IDS. Nevertheless, when Fe:IDS was
292 investigated (0.1 mM, molar ratio Fe:IDS = 1:1, $\text{H}_2\text{O}_2 = 50 \text{ mg L}^{-1}$), a lower efficiency in the
293 degradation of the target PCs was observed. Namely, SMX, CBZ and TMP were reduced up to 69%,
294 51% and 55%, respectively, after 180 min (12.8 kJ L^{-1}) (Table 2). Noteworthy, the concentration of

295 dissolved iron decreased faster in Fe:EDDS based SPF experiment. Indeed, iron almost totally
 296 precipitated (3 mg L⁻¹, Figure S1) after 60 min (Q_{uv}= 4.2 kJ L⁻¹), compared to Fe:IDS based SPF
 297 experiment (2.4 mg L⁻¹, Figure S1).

298 Iron precipitation resulted in a higher increase in wastewater turbidity for the Fe:EDDS complex
 299 (from 0.5 to 3.0 NTU after 60 min) compared to the Fe: IDS complex (from 0.5 to 1.1 NTU). Possibly
 300 the slower activity of the Fe:IDS complex resulted in a lower ROS production rate with a consequent
 301 reduced degradation of the ligand which finally keeps the iron in the dissolved phase longer. This
 302 ligand, like EDDS, can play a competing role for oxidating species at the same time. Lastly, reducing
 303 Fe concentration from 0.1 mM to 0.05 mM led to poor outcomes, as a consequence of the reduced
 304 production of radicals involved in the oxidation of the target PCs.

305

306 **Table 2.** Effect of Fe concentration and Fe:L ratio on the PCs removal efficiency. H₂O₂=1.47 mM, alkalinity=75 mg L⁻¹,
 307 Q_{uv}=12.9 kJ L⁻¹ (180 min).

Catalyst	Fe ³⁺ , mM	Fe:L ratio	TMP removed, %	CBZ removed, %	SMX removed, %
Fe:EDDS	0.05	1:1	38.4	19.5	40.7
	0.1	1:1	75.5	76.5	82
	0.1	1:1.5	48.1	43.7	55
	0.2	1:1	50.3	56.6	67.2
Fe:IDS	0.05	1:1	15.7	20.2	20.6
	0.1	1:1	55.2	50.6	69.4
	0.1	1:1.5	39.8	37.5	43.4
	0.2	1:1	39.6	37.6	52.1

308

309 **3.2 Effect of SPF on pathogens inactivation: comparison with sunlight/H₂O₂ process**

310 After the working conditions of SPF were optimized in terms of PCs removal (Fe:L = 0.1:0.1 mM),
 311 the effect of these conditions on *E. coli*, *C. perfringens* and coliphages (somatic and F-plus)
 312 inactivation was investigated. The target pathogens for disinfection's performance evaluation were
 313 selected according to the new EU regulation on wastewater reuse (EU 2020/741). The SPF process

314 was also compared with the sunlight/H₂O₂ process as a benchmark disinfection process. While
315 sunlight/H₂O₂ process poorly affects the PCs decomposition because of the poor generation of HO•
316 under natural solar radiation (Giannakis et al., 2016a; Moreira et al., 2018; Berruti et al., 2022;
317 Michael et al., 2020), it is an effective disinfection process (Ferro et al., 2015; García-Gil et al., 2022).
318 SPF with the two catalysts (Fe:IDS and Fe:EDDS) showed opposite behaviors for pathogens
319 inactivation with respect to what observed for PCs removal (Figure 2; Table S1-S3). Quite
320 surprisingly, Fe:EDDS (Figure 2a) resulted in reduced disinfection efficiency compared to Fe:IDS
321 counterpart (Figure 2b). Noteworthy, SPF with Fe:IDS allowed to achieve more than four log units
322 inactivation as well as to decrease residual *E. coli* concentration below the limit set by EU regulation
323 for wastewater reuse for class A water (10 CFU 100 mL⁻¹) in 180 min treatment (Q_{uv}=15.9 kJ L⁻¹).
324 On the opposite, SPF with Fe:EDDS resulted in a comparable poor efficiency with nearly two log
325 units inactivation, but consistent with previous results (Maniakova et al., 2021b).
326 The only apparent contradictory outcomes for Fe:IDS and Fe:EDDS based SPF processes in the
327 disinfection experiments, if compared with those obtained for the PCs removal, actually can be
328 explained as follows. While PCs degradation is a process almost exclusively dependent on the amount
329 of produced radical species, a different scenario takes place in the disinfection process. Indeed, it is
330 widely reported in the scientific literature how an important role in bacteria inactivation is played not
331 only by the radical species produced through the external SPF process, which damage the cell wall,
332 but even by the intracellular photo-Fenton mechanism triggered by the solar radiation (Fisher et al.,
333 2014; Giannakis et al., 2016a; Giannakis et al., 2016b; Giannakis et al., 2018; García-Gil et al., 2022;
334 Giannakis et al., 2022). The internal photo-Fenton reaction takes place thanks to H₂O₂ permeating the
335 cell membrane reacting with the bioavailable and externally added iron ions. Indeed, in Fe:EDDS
336 based SPF, the significantly higher consumption of H₂O₂ and the faster iron precipitation (Figure S3),
337 due to the degradation of the chelating agent, resulted in a higher turbidity (3 NTU) compared to
338 Fe:IDS tests (1.1 NTU). Presumably, the higher turbidity in Fe:EDDS tests acted as a screen for

339 sunlight, reducing its penetration inside bacteria cells and consequently resulting in a less effective
340 internal photo-Fenton mechanism.

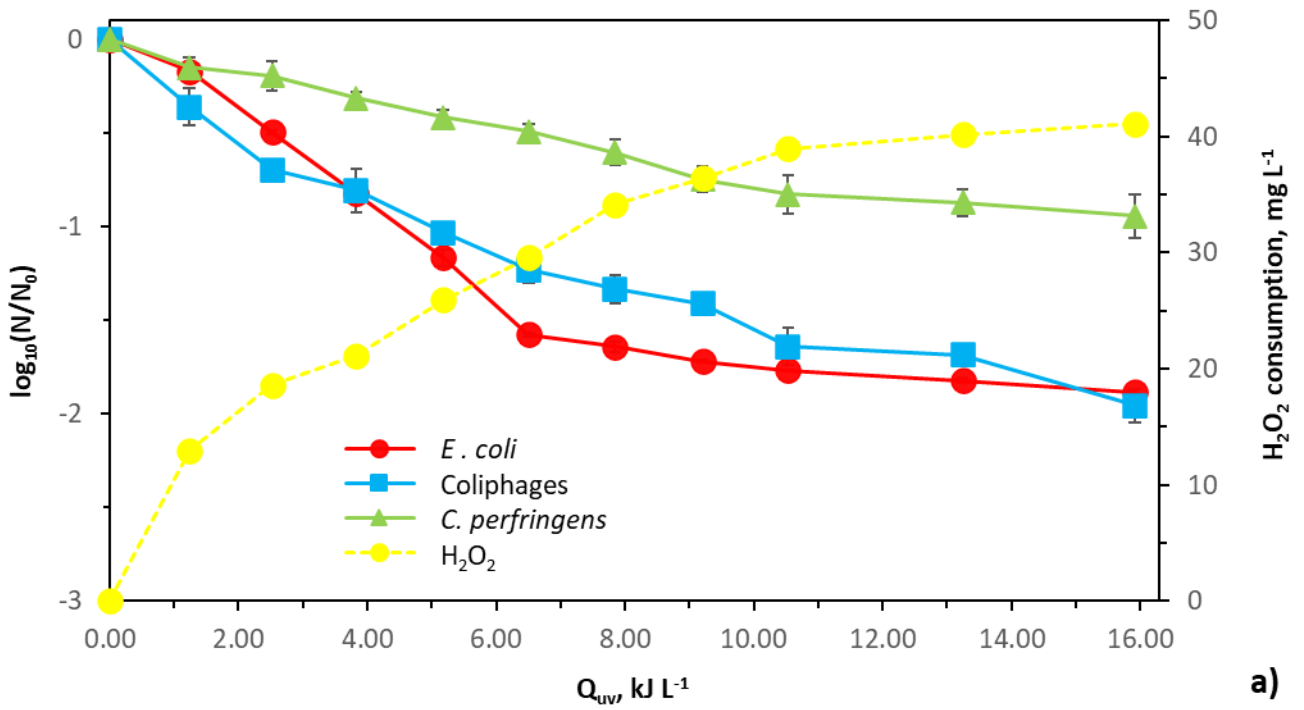
341 Interestingly, SPF with Fe:IDS was also more effective than sunlight/H₂O₂ process in *E. coli*
342 inactivation (Figure 2b and 2c, 3.3 log units inactivation). Consistently, sunlight/H₂O₂ process
343 performed better than Fe:EDDS based SPF process (Figure 2a and 2c), confirming previous literature
344 results (Maniakova et al., 2021b).

345 The inactivation efficiency of sunlight/H₂O₂ is mainly due to the aforementioned intracellular photo-
346 Fenton process, while in SPF this mechanism is coupled to the extracellular production of HO• and
347 other radical species that strongly contribute to membrane damaging, favoring the permeation of
348 H₂O₂ and Fe ions inside the cells (Rommozzi et al., 2020). For this reason, the lower reactivity of
349 Fe:IDS was found to be an advantage for the disinfection process. The lower production of HO• results
350 in a reduced degradation of the chelating agent with a lower turbidity of the aqueous matrix which,
351 in addition to the residual concentration of H₂O₂ (Figure 2b), make the internal photo-Fenton reaction
352 more effective. In summary, the three processes were found to be effective in *E. coli* inactivation in
353 the order: Fe:IDS based SPF > sunlight/H₂O₂ > Fe:EDDS based SPF.

354 At the same time, the effect of solar driven AOPs on the inactivation of other pathogens relevant for
355 the new EU regulation on wastewater reuse, namely *C. perfringens* and coliphages (somatic and F-
356 plus), was investigated. The order of inactivation of the target pathogens by Fe:IDS based SPF and
357 sunlight/H₂O₂ process was *E. coli* (under the DL of 1 CFU 100 mL⁻¹) > coliphages > *C. perfringens*,
358 while for Fe:EDDS the following order was observed: coliphages > *E. coli* > *C. perfringens* (Figure 2a,
359 3b and 3c). According to the scientific literature, differences occur between bacterial and viral
360 disinfection for SPF processes, with internal photo-Fenton playing a key-role in the disinfection for
361 bacteria and external ROS induced damage being the main pathway for inactivation of viruses.
362 Moreover, bacteriophages are more susceptible than bacteria to oxidation damage (Carratalà et al.,
363 2016; Giannakis et al., 2018). Again, Fe:IDS based SPF proved to be more effective than
364 sunlight/H₂O₂ and Fe:EDDS based SPF in coliphages inactivation. The high susceptibility of

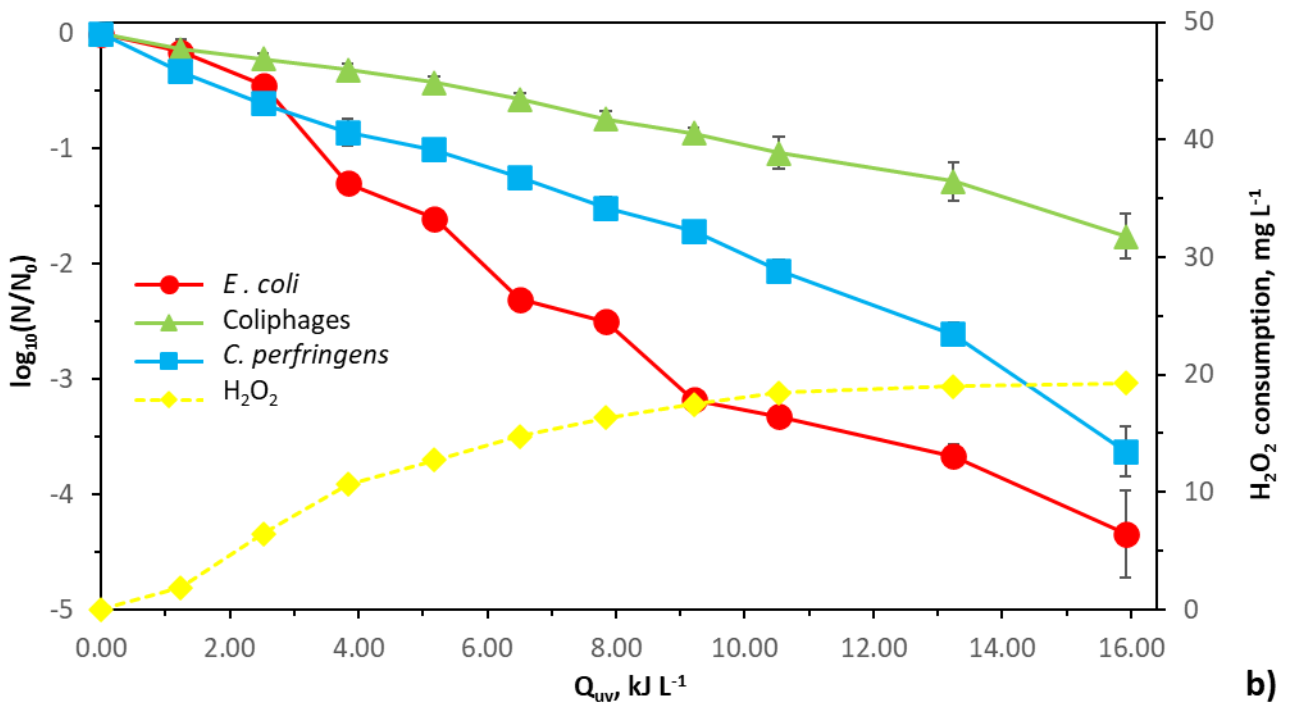
365 coliphages to oxidative damage explains the better performance of the Fe:IDS based SPF compared
366 to sunlight/H₂O₂. At the same time, the result seems contradictory considering that Fe:EDDS is able
367 to produce more radical species. A possible explanation can be found in the residual concentration of
368 H₂O₂ always higher in the SPF with Fe:IDS than in the SPF with Fe:EDDS. Furthermore, a strong
369 correlation among host bacteria abundance and bacteriophages resistance exists, according to the
370 literature; in particular, the more damaged the *E. coli*, the less the probability for coliphages to
371 continue their life-cycle (Voumard et al., 2019). Therefore, coliphages inactivation is directly
372 correlated to other bacteria inactivation. Moreover, the lesser precipitation of iron showed by Fe:IDS
373 based SPF (Figure S3) allows sunlight to play an important role in the disinfection. The important
374 role played by sunlight for viruses' disinfection has been clearly described in literature (Silverman et
375 al., 2019), therefore an iron complex both able to generate radical species, and stable enough to delay
376 iron precipitation and turbidity increasing, is desirable for bacteriophages inactivation.

377 Lastly, in all the processes *C. perfringens* resulted to be the most resistant pathogen. *C. perfringens*
378 is a gram-positive bacterium and, according to the scientific literature gram-negative and gram-
379 positive bacteria are characterized by different susceptibility to AOPs (Van Grieken et al., 2010;
380 Rodríguez-Chueca et al., 2013). Indeed, gram-negative (e.g., *E. coli*) ones bear an outer
381 lipopolysaccharidic membrane, which surrounds a thin peptidoglycan layer and an inner cytoplasmic
382 membrane (Silhavy et al., 2010). Instead, the gram-positive bacteria own a thicker layer of
383 peptidoglycans (Kloos et al., 1999). This difference in membrane composition can affect the cell
384 permeability (Frallicciardi et al., 2022), making the microorganism membrane more or less likely to
385 be penetrated by chemical compounds and/or hardly to resist to ROS attacks. In addition, a serious
386 threat posed by *C. perfringens* consists in being a spore-forming bacterium, able to generate resistant
387 forms (endospores) to protect themselves from adverse chemical-physical conditions as the presence
388 of ROS (Granger et al., 2011). In fact, spores are particularly resistant to SPF process (Kokkinos et
389 al., 2021).



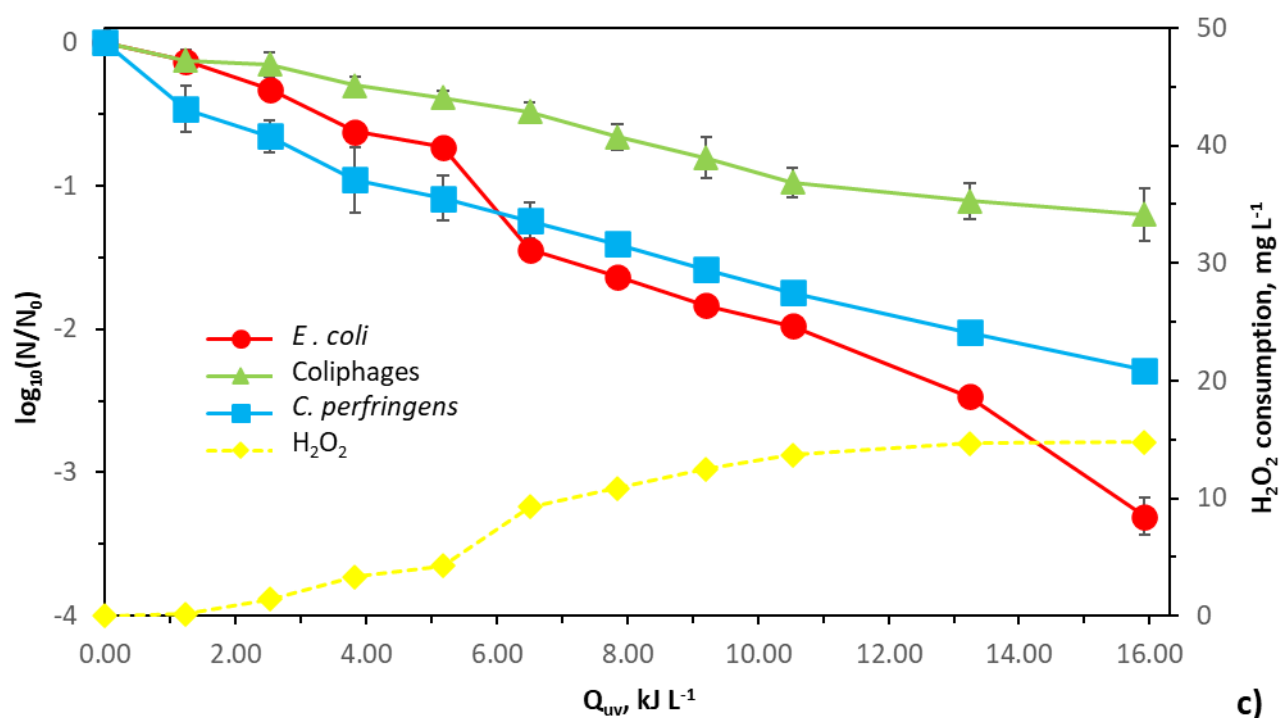
390

a)



391

b)



393

394 **Figure 2.** Inactivation of *E. coli*, coliphages and *C. perfringens* by Fe:EDDS based SPF (a), Fe:IDS based SPF (b) and
 395 sunlight/H₂O₂ process (c). Total time=180 min; H₂O₂=1.47 mM, Fe:L=0.1 mM:0.1 mM.

396

397 3.3 Sequential treatment: Sunlight/H₂O₂-SPF

398 Sunlight/H₂O₂ resulted more effective as disinfection process compared to Fe:EDDS based SPF
 399 (Figure 2a and 2c). On the other hand, it is quite ineffective in the PCs degradation, being not able to
 400 generate a sufficient amount of radicals unlike of SPF (Michael et al., 2020; Maniakova et al., 2021b).
 401 Therefore, Maniakova et al. investigated for the first time the sequential combination of sunlight/H₂O₂
 402 and SPF with Fe:EDDS obtaining simultaneous PCs removal and disinfection in real urban
 403 wastewater (Maniakova et al., 2022b). In our study, Fe:EDDS and Fe:IDS were also compared on
 404 their effects on PCs and pathogens in the sequential sunlight/H₂O₂-SPF treatment for the first time. For
 405 all the sequential treatment experiments, the total time remained unchanged (180 min), while the SPF
 406 phase lasted 120 min (about 8 kJ L⁻¹) to achieve a satisfactory PCs removal (limiting factor in the
 407 combination of sunlight/H₂O₂ and SPF) according to what was obtained from the previous
 408 experiments (Figure 1; Figure S1).

409 **3.3.1 PCs removal**

410 As PCs removal is of concern, sequential treatment with Fe:IDS was less efficient than the combined
411 process with Fe:EDDS (Figure 3a and 3b), consistently with the previous results on the application
412 of SPF as stand-alone process (Figure S1). In details, the average PCs removal was around 61% for
413 the sequential sunlight/H₂O₂-Fe:EDDS based SPF process, while for the Fe:IDS based SPF only 47%
414 was reached. Obviously, as in the early 60 min ($Q_{uv}= 4.2 \text{ kJ L}^{-1}$) the two conditions tested coincide
415 (sunlight/H₂O₂), sequential treatments differ only for the chelating agent used in the last 120 min (Q_{uv}
416 $\approx 9 \text{ kJ L}^{-1}$) of SPF. Sunlight/H₂O₂ had a limited effect on PCs removal (about 14%) according to
417 scientific literature (Michael et al., 2020; Maniakova et al., 2021b). Again, sequential treatment with
418 Fe:EDDS based SPF resulted more performant than sequential treatment with Fe:IDS based SPF for
419 the average PCs removal (61% vs 47%) (Figure 3). Recently, a study on the simultaneous removal of
420 PCs (five compounds at a concentration of 0.1 mg L^{-1}) and inactivation of pathogens (*E. coli* and
421 *Salmonella spp.*) by the sequential treatment sunlight/H₂O₂-Fe:EDDS based SPF reported an average
422 PCs removal of 60% (Maniakova et al., 2022b). While confirming the best performance of Fe:EDDS
423 in PCs removal, the sequential treatment was less effective than SPF stand-alone processes for both
424 catalysts (Figure 3, Figure S1). Since in the sequential treatment sufficient energy was accumulated
425 during the SPF phase compared to the previous results (about 9 kJ L^{-1}), the explanation for this
426 outcome may be due to the lower H₂O₂ concentration at the beginning of the SPF due to its
427 consumption during the preceding sunlight/H₂O₂ phase (Figure 3). This decreases the initial H₂O₂/Fe
428 ratio which can negatively affect the production of HO[•] and the PCs degradation, especially in
429 processes involving organic chelating agents (Lumbaque et al., 2019; Lin and Lin, 2021).
430 Furthermore, not only H₂O₂ can be an influencing factor, but also transformation products generated
431 by the sunlight/H₂O₂ phase can contribute to the matrix effect. Indeed, sunlight/H₂O₂ is not able to
432 mineralize the target contaminants which finally generate transformation products (Rizzo et al., 2019;

433 Michael et al. 2020). This implies that the PCs degraded during the sunlight/H₂O₂ phase are
 434 transformed in byproducts that can possibly affect the SPF reaction.

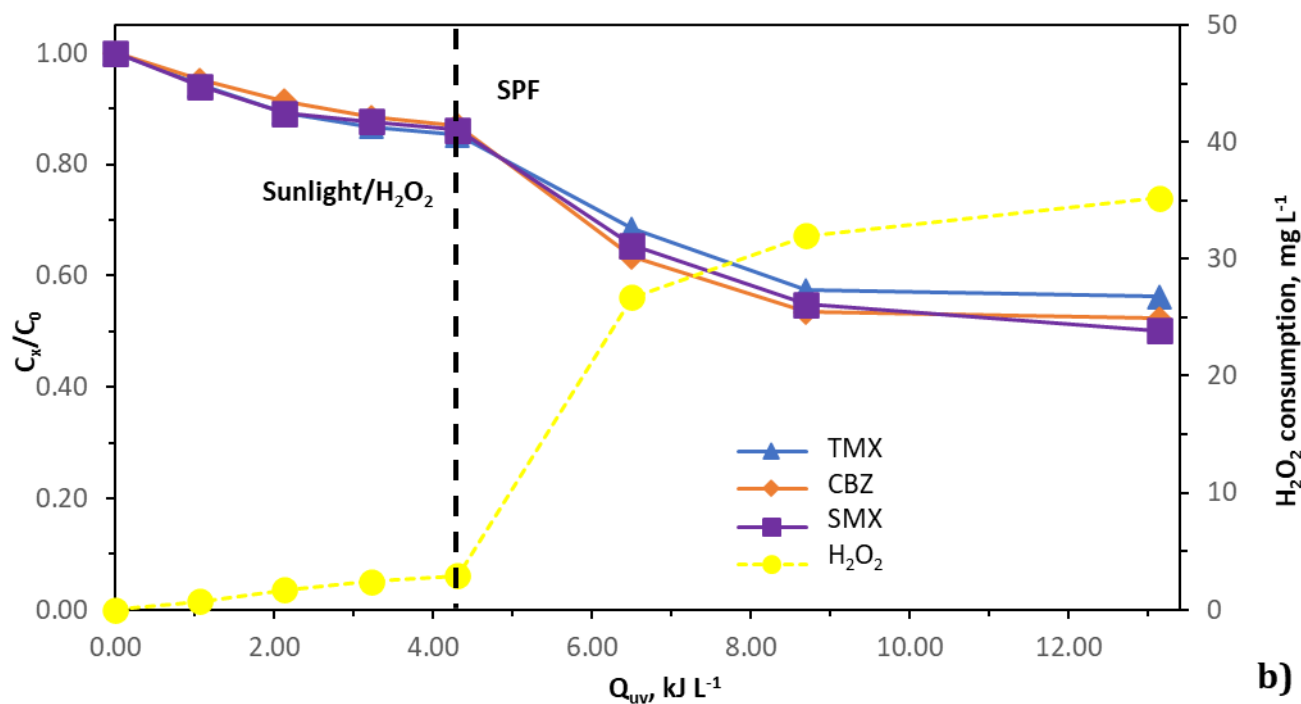
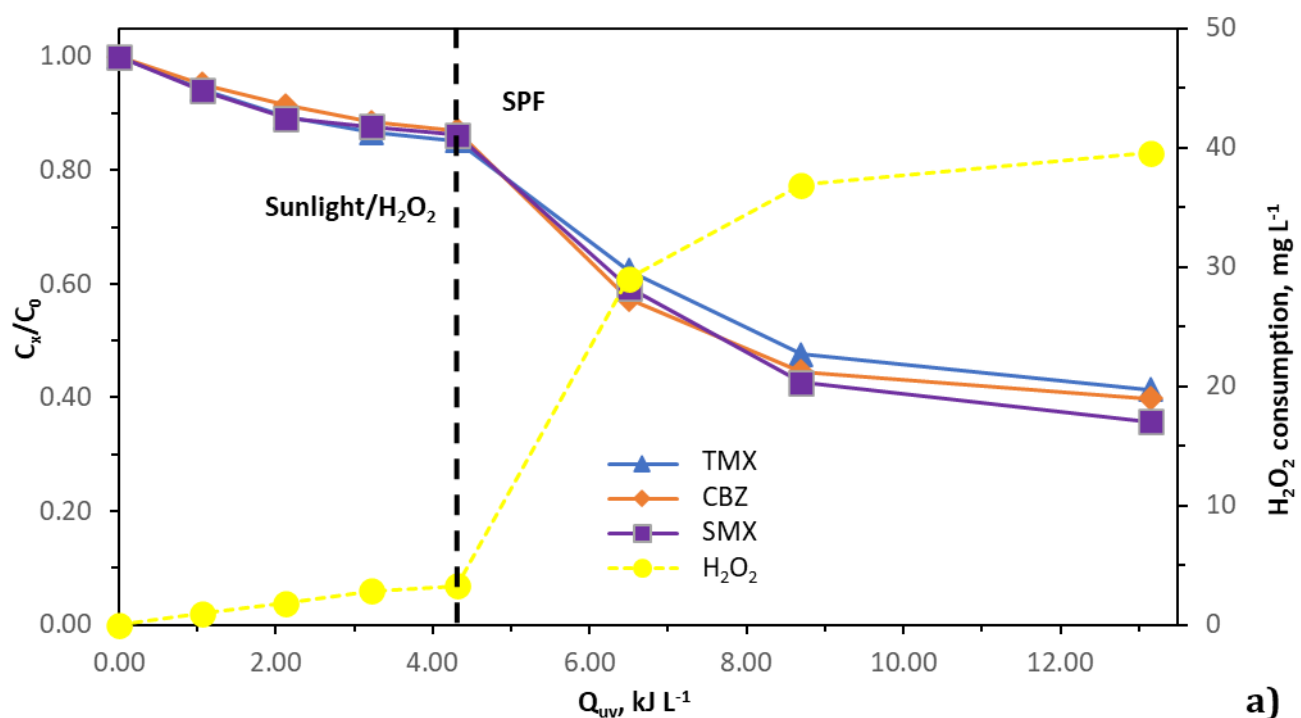


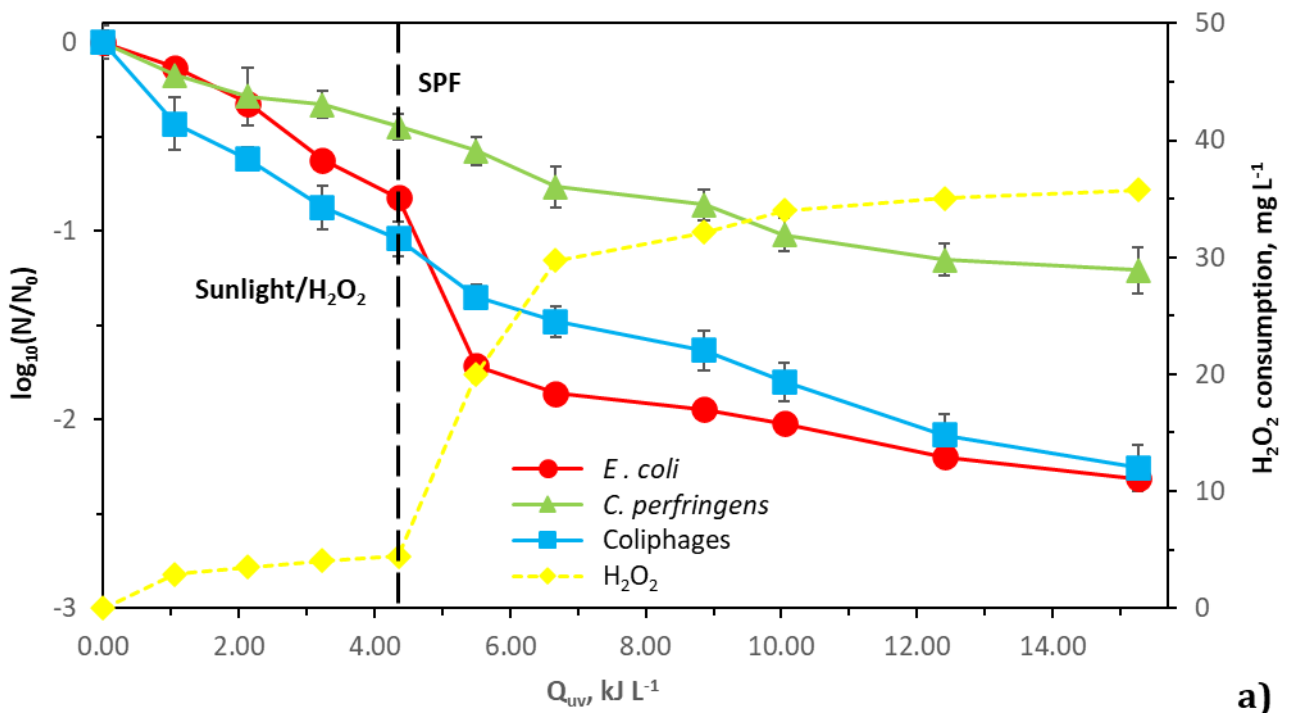
Figure 3. PCs removal by sequential treatment sunlight/H₂O₂ – Fe:EDDS (a) and sunlight/H₂O₂ – Fe:IDS (b). Total time=180 min; H₂O₂=1.47 mM; Fe:L=0.1 mM:0.1 mM.

440 3.3.2 Pathogens inactivation

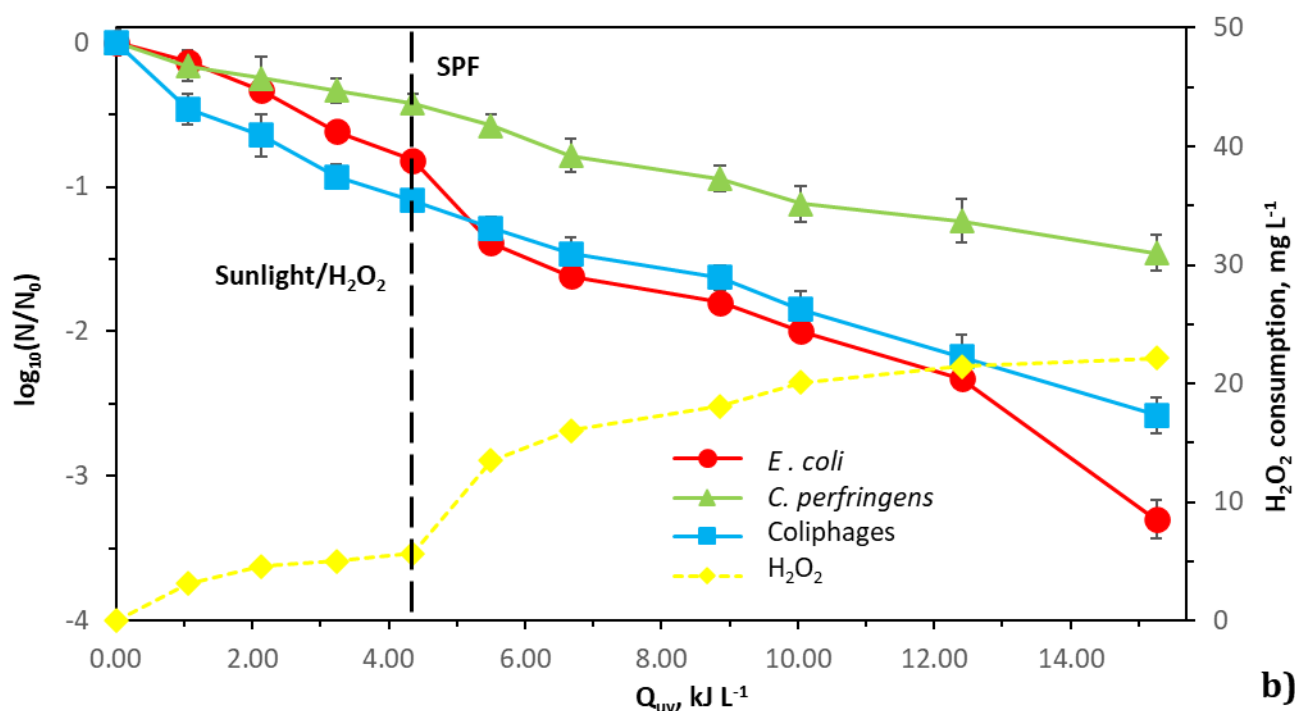
441 The effect on pathogens inactivation was also evaluated for sequential treatment sunlight/H₂O₂-SPF
442 (Figure 4; Table S4-S5). In sequential treatment, the Fe:IDS complex led to higher disinfection
443 efficiencies than the Fe:EDDS complex for all pathogens (3.4 vs 2.3 log reduction for *E. coli*, 2.6 vs
444 2.3 log reduction for coliphages, 1.5 vs 1.2 log reduction for *C. perfringens*, respectively). For both
445 chelating agents, contributions to the disinfection can be considered to stem from two separate steps:
446 firstly, sunlight/H₂O₂, then Fe:L based SPF. In the common first step, as previously discussed,
447 disinfection is driven by an internal photo-Fenton process. On the opposite, in the second step, two
448 pathways are possible. Consistently with the discussion about the effect of SPF on pathogens
449 inactivation, after adding Fe:IDS (Figure 4b), disinfection is driven by intracellular photo-Fenton
450 conjugated with extracellular photo-Fenton. With Fe:EDDS (Figure 4a), H₂O₂ and Fe ions are quickly
451 consumed outside the cells, the turbidity increases faster, thus making the intracellular photo-Fenton
452 mechanism less relevant compared to Fe:IDS. The progressive and almost total consumption of H₂O₂
453 in the Fe:EDDS based SPF phase (Figure 4a) led to a reduction in the pathogens inactivation rate. In
454 contrast, in sequential treatment with Fe:IDS based SPF, the pathogen inactivation rate continued to
455 increase, consistently with the high H₂O₂ availability until the end of treatment. Moreover, the
456 sequential treatment with Fe:IDS based SPF (Figure 4b) showed a lower efficiency than its
457 corresponding SPF (Figure 2b) as a stand-alone process (3.4 vs 4.3 log reduction for *E. coli*, 2.6 vs
458 3.6 log reduction for coliphages, 1.5 vs 1.8 log reduction for *C. perfringens*). This worsening confirms
459 the hypothesis on the disinfection mechanisms involved in the Fe:IDS based SPF. Indeed, by coupling
460 the sunlight/H₂O₂ process to SPF, the time in which both mechanisms (internal and external photo-
461 Fenton) coexist is reduced (from 180 min to 120 min). On the other hand, and according to the only
462 previous work reporting this comparison (Maniakova et al., 2021b), the sequential treatment with
463 Fe:EDDS based SPF (Figure 4a) showed a higher efficiency than its corresponding SPF (Figure 2a)
464 as a stand-alone process (2.3 vs 1.9 log reduction for *E. coli*; 2.3 vs 2 log reduction for coliphages,

465 1.2 vs 0.9 log reduction for *C. perfringens*). The increased pathogen inactivation in this case may be
 466 due to cell wall weakening caused by the internal photo-Fenton during the sunlight/H₂O₂ phase. This
 467 had a beneficial effect especially on *E. coli* inactivation during the SPF. Indeed, *E. coli* is the only
 468 one of the three pathogens to undergo an increase in disinfection rate after SPF started (Figure 4a).
 469 This result can be explained through the higher susceptibility of this bacterium in being permeated
 470 and damaged by H₂O₂ due to the weaker cell wall compared to *C. perfringens* (Van Grieken et al.,
 471 2010; Rodríguez-Chueca et al., 2013; Frallicciardi et al., 2022).

472



473



474

475 **Figure 4.** Inactivation of *E. coli*, coliphages and *C. perfringens* by sequential treatment: sunlight/H₂O₂ – SPF with

476 Fe:EDDS (a) and Fe:IDS (b). Total time=180 min; H₂O₂=1.47 mM; Fe:L=0.1 mM:0.1 mM.

477 Conclusions

478 In this study, the Fe:IDS complex as a catalyst for SPF process at natural pH was investigated for the
 479 first time as a tertiary treatment for wastewater reuse in agriculture applications. The Fe:IDS based
 480 SPF was compared with the well-known Fe:EDDS based SPF and then with the sequential treatment
 481 configuration (sunlight/H₂O₂-SPF) in terms of pathogens (*E. coli*; *C. perfringens*; coliphages)
 482 inactivation and PCs (SMX, CBZ, TMP) removal from real secondary wastewater. Both Fe:L based
 483 SPF treatments were found to be effective in the simultaneous disinfection and PCs removal, but
 484 Fe:IDS based SPF resulted the best option for pathogens inactivation, allowing to meet the most
 485 stringent limit (Class A = 10 CFU/100 ml) for *E. coli* set by EU regulation for wastewater reuse
 486 (2020/441). Moreover, the process also affected *C. perfringens* and coliphages that are relevant for
 487 the wastewater treatment plant validation for wastewater reuse. On the other hand, Fe:IDS based SPF
 488 was found to be less effective for PCs degradation compared to Fe:EDDS based SPF. The main
 489 explanation for the differences between the two catalysts is that the lower reactivity of Fe:IDS results

490 in a reduced consumption of Fenton's reagents favouring both the intracellular and extracellular
491 photo-Fenton mechanisms for disinfection but lowering its PCs degradation potential. Noteworthy,
492 while for Fe:EDDS the sequential treatment increased the disinfection efficiency, for the Fe:IDS the
493 sunlight/H₂O₂ step was deleterious in terms of performances.
494 Considering its good all-round performance, but also IDS higher biodegradability, Fe:IDS can be an
495 attractive alternative option to Fe:EDDS in SPF process for the tertiary treatment of urban wastewater
496 in small WTPs, especially when more stringent limits on pathogens should be meet (as in the case of
497 the new EU regulation on wastewater reuse) and residual PCs in the effluent is consistent with the
498 corresponding treatment target.

499 **Acknowledgments**

500 This paper is supported by the PRIMA programme under grant agreement No 1822, project “Decision
501 support-based approach for Sustainable Water reuse application in Agricultural Production –
502 DSWAP”. The PRIMA programme is supported by the European Union. Moreover, the support from
503 the staff of Sistemi Salerno S.p.A. and in particular that one of Dr. Osvaldo Agresti during wastewater
504 sampling was highly appreciated.

505 **References**

- 506 Baba, Y., Yatagai, T., Harada, T., Kawase, Y., 2015. Hydroxyl radical generation in the photo-Fenton
507 process: Effects of carboxylic acids on iron redox cycling. *Chem. Eng. J.* 277, 229-241. doi:
508 10.1016/j.cej.2015.04.103.
- 509 Berruti, I., Nahim-Granados, S., Abeledo-Lameiro, M. J., Oller, I., Polo-López, M. I., 2022. *Chem.*
510 *Eng. J. Adv.* 10, 100248. doi: 10.1016/j.cej.2022.100248.
- 511 Cabrera-Reina, A., Miralles-Cuevas, S., Sánchez Pérez, J.A., Salazar, R., 2021. Application of solar
512 photo-Fenton in raceway pond reactors: A review. *Sci. Total. Environ.*, 800, 149653.
513 doi:10.1016/j.scitotenv.2021.149653.

514 Cacace, D., Fatta-Kassinos, D., Manaia, C. M., Cytryn, E., Kreuzinger, N., Rizzo, L., Karaolia, P.,
515 Schwartz, T., Alexander, J.; Merlin, C., Garelick, H., Schmitt, H., De Vries, D., Schwermer, C. U.,
516 Meric, S., Ozkal, C. B., Pons, M.-N., Kneis, D., Berendonk, T. U., 2019. Antibiotic resistance genes
517 in treated wastewater and in the receiving water bodies: A pan-European survey of urban settings.
518 *Water Res.* 162, 320-330. doi: 10.1016/j.watres.2019.06.039.

519 Carra, I., Santos-Juanes, L., Ación Fernández, F. G., Malato S., Sánchez Pérez J. A., 2014. New
520 approach to solar photo-Fenton operation. Raceway ponds as tertiary treatment technology. *J. Hazard.*
521 *Mater.* 279, 322-329. doi: 10.1016/j.jhazmat.2014.07.010.

522 Carratalà, A., Calado, A. D., Mattle, M. J., Meierhofer, R., Luzi, S., Kohn, T., 2016. Solar
523 Disinfection of Viruses in Polyethylene Terephthalate Bottles. *Appl. Environ. Microbiol.* 82, 279-
524 288. doi: 10.1128/AEM.02897-15.

525 Christou, A., Karaolia, P., Hapeshi, E., Costas, M., Fatta-Kassinos, D., 2017. Long-term wastewater
526 irrigation of vegetables in real agricultural systems: Concentration of pharmaceuticals in soil, uptake
527 and bioaccumulation in tomato fruits and human health risk assessment. *Water Res.* 109, 24-34. doi:
528 10.1016/j.watres.2016.11.033.

529 Christou, A., Kyriacou, M. C., Georgiadou, E. C., Papamarkou, R., Hapeshi, E., Karaolia, P., Costas,
530 M., Fotopoulos, V., Fatta-Kassinos, D., 2019. Uptake and bioaccumulation of three widely prescribed
531 pharmaceutically active compounds in tomato fruits and mediated effects on fruit quality attributes.
532 *Sci. Total. Environ.*, 647, 1169-1178. doi: 10.1016/j.scitotenv.2018.08.053.

533 Clarizia, L., Russo, D., Di Somma, I., Marotta, R., Andreozzi, R., 2017. Homogeneous photo-Fenton
534 processes at near neutral pH: a review. *Appl. Catal. B Environ.* 209, 358–371.
535 doi:10.1016/j.apcatb.2017.03.011.

536 Cokesa, Z., Knackmuss, H. J., Rieger, P. G., 2004. Biodegradation of all stereoisomers of the EDTA
537 substitute iminodisuccinate by agrobacterium tumefaciens BY6 requires an epimerase and a
538 stereoselective C-N lyase. *Appl. Environ. Microbiol.* 70, 3941-3947. doi: 10.1128/AEM.70.7.3941-
539 3947.2004.

540 Comninellis, C., Kapalka, A., Malato, S., Parsons, S. A., Poullos, I., Mantzavinos, D., 2008.
541 Advanced oxidation processes for water treatment: advances and trends for R&D. *J. Chem. Technol.*
542 *Biotechnol.* 83, 769-776. doi: 10.1002/jctb.1873.

543 De La Cruz, N., Esquius, L., Grandjean, D., Magnet, A., Tungler, A., de Alencastro, L. F., Pulgarín,
544 C., 2013. Degradation of emergent contaminants by UV, UV/H₂O₂ and neutral photo-Fenton at pilot
545 scale in a domestic wastewater treatment plant. *Water Res.* 47, 5836-5845. doi:
546 10.1016/j.watres.2013.07.005.

547 De la Obra, I., Ponce-Robles L., Miralles-Cuevas S., Oller I., Malato, S., Sánchez Pérez, J.A., 2017.
548 Microcontaminant removal in secondary effluents by solar photo-Fenton at circumneutral pH in
549 raceway pond reactors, *Catal. Today* 287, 10–14. doi: 10.1016/j.cattod.2016.12.028.

550 Deng, Y. and Zhao, R., 2015. Advanced Oxidation Processes (AOPs) in Wastewater Treatment. *Curr.*
551 *Pollution Rep.* 1, 167-176. doi: 10.1007/s40726-015-0015-z.

552 Deviller, G., Lundy, L., Fatta-Kassinos, D., 2020. Recommendations to derive quality standards for
553 chemical pollutants in reclaimed water intended for reuse in agricultural irrigation *Chemosphere* 240,
554 124911. doi: 10.1016/j.chemosphere.2019.124911.

555 Faggiano, A., Ricciardi, M., Fiorentino, A., Cucciniello, R., Motta, O., Rizzo, L., Proto, A., 2022.
556 Combination of foam fractionation and photo-Fenton like processes for greywater treatment. *Sep.*
557 *Purif. Technol.* 293, 121114. doi: 10.1016/j.seppur.2022.121114.

558 Fatta-Kassinos, D., Kalavrouziotis, I. K., Koukoulakis, P. H., Vasquez, M. I., 2011. The risks
559 associated with wastewater reuse and xenobiotics in the agroecological environment. *Sci. Total.*
560 *Environ.* 409, 3555-3563. doi: 10.1016/j.scitotenv.2010.03.036.

561 Fatta-Kassinos, D., Costas, M., 2013. Wastewater reuse applications and contaminants of emerging
562 concern. *Environ. Sci. Pollut. Res.* 20, 3493-3495. doi: 10.1007/s11356-013-1699-5.

563 Ferro, G., Fiorentino, A., Alferez, M. C., Polo-López, M. I., Rizzo, L., Fernández-Ibáñez, P., 2015.
564 Urban wastewater disinfection for agricultural reuse: effect of solar driven AOPs in the inactivation
565 of a multidrug resistant *E. coli* strain. *Appl. Catal. B.*, 178, 65-73. doi: 10.1016/j.apcatb.2014.10.043.

566 Fiorentino, A., Cucciniello, R., Di Cesare, A., Fontaneto, D., Prete, P., Rizzo, L., Corno, G., Proto,
567 A., 2018. Disinfection of urban wastewater by a new photo-Fenton like process using Cu-
568 iminodisuccinic acid complex as catalyst at neutral pH. *Water Res.* 146, 206-215. doi:
569 10.1016/j.watres.2018.08.024.

570 Fiorentino, A., Esteban, B., Garrido-Cardenas, J. A., Kowalska, K., Rizzo, L., Aguera, A., Sánchez
571 Pérez, J. A., 2019. Effect of solar photo-Fenton process in raceway pond reactors at neutral pH on
572 antibiotic resistance determinants in secondary treated urban wastewater. *J. Hazard Mater.* 378,
573 120737. doi: 10.1016/j.jhazmat.2019.06.014.

574 Fiorentino, A., Prete, P., Rizzo, L., Cucciniello, R., Proto, A., 2021. Fe³⁺-IDS as a new green catalyst
575 for water treatment by photo-Fenton process at neutral pH. *J. Environ. Chem. Eng.* 9(6), 106802. doi:
576 10.1016/j.jece.2021.106802.

577 Frallicciardi, J., Melcr, J., Siginou, P., Marrink, S. J., Poolman, B., 2022. Membrane thickness, lipid
578 phase and sterol type are determining factors in the permeability of membranes to small solutes. *Nat.*
579 *Commun.* 13, 1605. doi: 10.1038/s41467-022-29272-x.

580 García-Gil, A., Feng, L., Moreno-SanSegundo, J., Giannakis, S., Pulgarín, C., Marugan, J., 2022.
581 Mechanistic modelling of solar disinfection (SODIS) kinetics of *Escherichia coli*, enhanced with
582 H₂O₂ – Part 2: Shine on you, crazy peroxide. *Chem. Eng. J.*, 439, 135783.
583 doi:10.1016/j.cej.2022.135783.

584 Giannakis, S., Polo López, M. I., Spuhler, D., Sánchez Pérez, J. A., Ibáñez, P. F., Pulgarin, C., 2016a.
585 Solar disinfection is an augmentable, in situ-generated photo-Fenton reaction—Part 1: A review of
586 the mechanisms and the fundamental aspects of the process. *Appl. Catal. B* 199, 199-223. doi:
587 10.1016/j.apcatb.2016.06.009.

588 Giannakis, S., Polo López, M. I., Spuhler, D., Sánchez Pérez, J. A., Ibáñez, P. F., Pulgarin, C., 2016b.
589 Solar disinfection is an augmentable, in situ-generated photo-Fenton reaction—Part 2: A review of
590 the applications for drinking water and wastewater disinfection. *Appl. Catal. B* 198, 431-446. doi:
591 10.1016/j.apcatb.2016.06.007.

592 Giannakis, S., Voumard, M., Rtimi, S., Pulgarin, C., 2018. Bacterial disinfection by the photo-Fenton
593 process: Extracellular oxidation or intracellular photo-catalysis? *Appl. Catal. B* 227, 285-295. doi:
594 10.1016/j.apcatb.2018.01.044.

595 Giannakis, S., Gupta, A., Pulgarin, C., Imlay, J., 2022. Identifying the mediators of intracellular *E.*
596 *coli* inactivation under UVA light: The (photo) Fenton process and singlet oxygen. *Water Res.* 221,
597 118740. doi: 10.1016/j.watres.2022.118740.

598 Granger, A. C., Gaidamakova, E. K., Matrosova, V. Y., Daly, M. J., Setlow, P., 2011. Effects of Mn
599 and Fe Levels on *Bacillus subtilis* Spore Resistance and Effects of Mn²⁺, Other Divalent Cations,
600 Orthophosphate, and Dipicolinic Acid on Protein Resistance to Ionizing Radiation. *Appl Environ*
601 *Microbiol.* 77, 32-40. doi: 10.1128/AEM.01965-10.

602 Gualda-Alonso, E., Soriano-Molina, P., Casas López, J. L., García Sánchez, J. L., Plaza-Bolaños, P.,
603 Agüera, A., Sánchez Pérez, J. A., 2022. Large-scale raceway pond reactor for CEC removal from
604 municipal WWTP effluents by solar photo-Fenton. *Appl. Catal. B.* 319, 121908. doi:
605 10.1016/j.apcatb.2022.121908.

606 Hossain, K. A., Roy, K., 2018. Chemometric modeling of aquatic toxicity of contaminants of
607 emerging concern (CECs) in *Dugesia japonica* and its interspecies correlation with daphnia and fish:
608 QSTR and QSTTR approaches. *Ecotoxicol. Environ. Saf.* 166, 92-101. doi:
609 10.1016/j.ecoenv.2018.09.068.

610 Ji, Y., Dong, C., Kong, D., Lu, J., Zhou, Q., 2015. Heat-activated persulfate oxidation of atrazine:
611 Implications for remediation of groundwater contaminated by herbicides, *Chem. Eng. J.* 263, 45–54,
612 doi: 10.1016/j.cej.2014.10.097

613 Kokkinos, P., Venieri, D., Mantzavinos, D., 2021. Advanced Oxidation Processes for Water and
614 Wastewater Viral Disinfection. A Systematic Review. *Food Environ Virol.* 13, 283-302. doi:
615 10.1007/s12560-021-09481-1.

616 Krzeminski, P., Tomei, M.C., Karaolia, P., Langenhoff, A., Almeida, C.M.R., Felis, E., Gritten, F.,
617 Andersen, H.R., Fernandes, T., Manaia, C.M., Rizzo, L., Fatta-Kassinos, D., 2019. Performance of
618 secondary wastewater treatment methods for the removal of contaminants of emerging concern
619 implicated in crop uptake and antibiotic resistance spread: A review. *Sci. Total Environ.* 648, 1052-
620 1081. doi: 10.1016/j.chemosphere.2011.09.006.

621 Kummu, M., Guillame, J. H. A., De Moel, H., Eisner, S., Flörke, M., 2016. The world's road to water
622 scarcity: shortage and stress in the 20th century and pathways towards sustainability. *Scientific*
623 *Reports* 6. 38495, doi:10.1038/srep38495.

624 Lin, H. H., Lin, A. Y., 2021. Solar photo-Fenton oxidation of cytostatic drugs via Fe(III)-EDDS at
625 circumneutral pH in an aqueous environment. *Journal of Water Process Engineering*, 41, 102066.
626 doi:10.1016/j.jwpe.2021.102066

627 Lofrano, G., Faiella, M., Carotenuto, M., Murgolo, S., Mascolo, G., Pucci, L., Rizzo, L., 2021. Thirty
628 contaminants of emerging concern identified in secondary treated hospital wastewater and their
629 removal by solar Fenton (like) and sulphate radicals-based advanced oxidation processes. *J. Environ.*
630 *Chem. Eng.* 9, 106614. doi: 10.1016/j.jece.2021.106614.

631 Lumbaqué, E. C., Araújo, D. S., Klein, T. M., Tiburtius, E. R. L. Argüello, J., Sirtori, C., 2019. Solar
632 photo-Fenton-like process at neutral pH: Fe(III)-EDDS complex formation and optimization of
633 experimental conditions for degradation of pharmaceuticals. *Catal. Today* 328, 259-266. doi:
634 10.1016/j.cattod.2019.01.006

635 Malato, S., Blanco, J., Campos, A., Cáceres, J., Guillard, C., Herrmann, J. M., Fernández-Alba, A.
636 R., 2003. Effect of operating parameters on the testing of new industrial titania catalysts at solar pilot
637 plant scale. *Appl. Catal. B: Environ.* 42, 349-357. doi: 10.1016/S0926-3373(02)00270-9.

638 Maniakova, G., Kowalska, K., Murgolo, S., Mascolo, G., Libralato, G., Lofrano, G., Sacco, O.,
639 Guida, M., Rizzo, L., 2020. Comparison between heterogeneous and homogeneous solar driven
640 advanced oxidation processes for urban wastewater treatment: Pharmaceuticals removal and toxicity.
641 *Sep. Purif. Technol.* 236, 116249. doi: 10.1016/j.seppur.2019.116249.

642 Maniakova, G., Salmerón, I., Nahim-Granados, S., Malato, S., Oller, I., Rizzo, L., Polo-López, M. I.,
643 2021a. Sunlight advanced oxidation processes vs ozonation for wastewater disinfection and safe
644 reclamation. *Sci. Total Environ.* 787, 147531. doi: 10.1016/j.scitotenv.2021.147531.

645 Maniakova, G., Salmerón, I., Polo-López, M. I., Oller, I., Rizzo, L., Malato, S., 2021b. Simultaneous
646 removal of contaminants of emerging concern and pathogens from urban wastewater by
647 homogeneous solar driven advanced oxidation processes. *Sci. Total Environ.* 766, 144320. doi:
648 10.1016/j.scitotenv.2020.144320.

649 Maniakova, G., Salmerón, I., Aliste, M., Polo-López, M. I., Oller, I., Malato, S., Rizzo, L., 2022a.
650 Solar photo-Fenton at circumneutral pH using Fe(III)-EDDS compared to ozonation for tertiary
651 treatment of urban wastewater: Contaminants of emerging concern removal and toxicity assessment.
652 *Chem. Eng. J.* 431, 133474. doi: 10.1016/j.cej.2021.133474.

653 Maniakova, G., Polo-López, M. I., Oller, I., Abeledo-Lameiro, M. J., Malato, S., Rizzo, L., 2022b.
654 Simultaneous disinfection and microcontaminants elimination of urban wastewater secondary

655 effluent by solar advanced oxidation sequential treatment at pilot scale. *J. Hazard Mater.* 2022, 436,
656 129134. doi: 10.1016/j.jhazmat.2022.129134.

657 Mekonnen, M. M., Hoekstra, A. Y., 2016. Four Billion People Facing Severe Water Scarcity. *Sci.*
658 *Adv.* 2, doi:10.1126/sciadv.1500323.

659 Michael, S. G., Michael-Kordatou, I., Nahim-Granados, S., Polo-López, M. I., Rocha, J., Martínez-
660 Piernas, A. B., Fernández-Ibáñez, P., Agüera, A., Manaia, C. M., Fatta-Kassinos, D., 2020.
661 Investigating the impact of UV-C/H₂O₂ and sunlight/H₂O₂ on the removal of antibiotics, antibiotic
662 resistance determinants and toxicity present in urban wastewater. *Chem. Eng. J.* 388, 124383. doi:
663 10.1016/j.cej.2020.124383.

664 Miralles-Cuevas, S., Audino, F., Oller, I., Sánchez-Moreno, R., Sánchez Pérez, J. A., Malato, S.,
665 2014. Pharmaceuticals removal from natural water by nanofiltration combined with advanced tertiary
666 treatments (solar photo-Fenton, photo-Fenton-like Fe(III)–EDDS complex and ozonation). *Sep.*
667 *Purif. Technol.* 122, 515-522. doi: 10.1016/j.seppur.2013.12.006.

668 Miralles-Cuevas, S., Oller, I., Ruíz-Delgado, A., Cabrera-Reina, A., Cornejo-Ponce, L., Malato, S.,
669 2019. EDDS as complexing agent for enhancing solar advanced oxidation processes in natural water:
670 effect of iron species and different oxidants. *J. Hazard. Mater.* 372, 129-136. doi:
671 10.1016/j.jhazmat.2018.03.018.

672 Moreira, N. F. F., Narciso-da-Rocha, C., Polo-López, M. I., Pastrana-Martínez, L. M., Faria, J. L.,
673 Manaia, C. M., Fernández-Ibáñez, P., Nunes, O. C., Silva, A. M. T., 2018. Solar treatment (H₂O₂,
674 TiO₂-P25 and GO-TiO₂ photocatalysis, photo-Fenton) of organic micropollutants, human pathogen
675 indicators, antibiotic resistant bacteria and related genes in urban wastewater. *Water Res.* 135, 195-
676 206. doi: 10.1016/j.watres.2018.01.064.

677 O’Dowd, K., Pillai, S. C., 2020. Photo-Fenton disinfection at near neutral pH: Process, parameter
678 optimization and recent advances. *J. Environ. Chem. Eng.* 8, 104063, doi:
679 10.1016/j.jece.2020.104063.

680 Oller, I., Malato, S., 2021. Photo-Fenton applied to the removal of pharmaceutical and other
681 pollutants of emerging concern. *Curr. Opin. Green Sustain. Chem.* 29, 100458. doi:
682 10.1016/j.cogsc.2021.100458.

683 Papoutsakis, S., Brites-Nóbrega, F. F., Pulgarin, C., Malato, S., 2015. Benefits and limitations of
684 using Fe(III)-EDDS for the treatment of highly contaminated water at near-neutral pH J. Photochem.
685 Photobiol. A 303, 1-7. doi: 10.1016/j.jphotochem.2015.01.013.

686 Pastorino, P., Ginebreda, A., 2021. Contaminants of Emerging Concern (CECs): Occurrence and Fate
687 in Aquatic Ecosystems. Int. J. Environ. Res. Public Health 18, 13401. doi: 10.3390/ijerph182413401.

688 Pignatello, J. J., Oliveros, E., MacKay, A., 2006. Advanced oxidation processes for organic
689 contaminant destruction based on the Fenton reaction and related chemistry. Crit. Rev. Environ. Sci.
690 Technol. 36, 1-84. doi: 10.1080/10643380500326564.

691 Prete, P., Fiorentino, A., Rizzo, L., Proto, A., Cucciniello, R., 2021. Review of aminopolycarboxylic
692 acids-based metal complexes application to water and wastewater treatment by (photo-)Fenton
693 process at neutral pH. Curr. Opin. Green Sustain. Chem. 28, 100451. doi:
694 10.1016/j.cogsc.2021.100451.

695 Prieto-Rodríguez, L., Oller, I., Klamerth, N., Agüera, A., Rodríguez, E. M., Malato, S., 2013.
696 Application of solar AOPs and ozonation for elimination of micropollutants in municipal wastewater
697 treatment plant effluents. Water Res. 47, 1521-1528. doi: 10.1016/j.watres.2012.11.002.

698 Regulation (EU) 2020/741 of the European parliament and of the council of 25 May 2020 on
699 minimum requirements for water reuse, Official Journal of the European Union L 177/32, 5.6.2020.

700 Rizzo, L., Krätke, R., Linders, J., Scott, M., Vighi, M., De Voogt, P., 2018. Proposed EU minimum
701 quality requirements for water reuse in agricultural irrigation and aquifer recharge: SCHEER
702 scientific advice. Curr. Opin. Environ. Sci. Health 2, 7-11. doi: 10.1016/j.coesh.2017.12.004.

703 Rizzo, L., Malato, S., Antakyali, D., Beretsou, V. G., Dolić, M. B., Gernjak, W., Heath, E., Ivancev-
704 Tumbas, I., Karaolia, P., Lado Ribeiro, A. R., Mascolo, G., McArdell, C. S., Schaar, H., Silva, A. M.
705 T., Fatta-Kassinos, D., 2019. Consolidated vs new advanced treatment methods for the removal of
706 contaminants of emerging concern from urban wastewater. Sci. Total Environ. 655, 986-1008. doi:
707 10.1016/j.scitotenv.2018.11.265.

708 Rizzo, L., Gernjak, W., Krzeminski, P., Malato, S., McArdell, C. S., Sanchez Perez, J. A., Schaar,
709 H., Fatta-Kassinos, D., 2020. Best available technologies and treatment trains to address current
710 challenges in urban wastewater reuse for irrigation of crops in EU countries. Sci. Total Environ. 710,
711 13612. doi: 10.1016/j.scitotenv.2019.136312.

712 Rizzo, L., 2022. Addressing main challenges in the tertiary treatment of urban wastewater: are
713 homogeneous photodriven AOPs the answer?. *Environ. Sci.: Water Res. Technol.* 8, 2145-2169. doi:
714 10.1039/D2EW00146B.

715 Rodríguez-Chueca, J., Polo-López, M. I., Mosteo, R., Ormad, M. P., Fernández-Ibáñez, P., 2014.
716 Disinfection of real and simulated urban wastewater effluents using a mild solar photo-Fenton. *Appl.*
717 *Catal. B.* 150-151, 619-629. doi: 10.1016/j.apcatb.2013.12.027.

718 Rommozzi, E., Giannakis, S., Giovannetti, R., Vione, D., Pulgarin, C., 2020. Detrimental vs.
719 beneficial influence of ions during solar (SODIS) and photoFenton disinfection of *E. coli* in water:
720 (Bi)carbonate, chloride, nitrate and nitrite effects. *Appl. Catal. B.* 270, 118877. doi:
721 10.1016/j.apcatb.2020.118877.

722 Sánchez Pérez, J.A., Arzate, S., Soriano-Molina, P., García Sánchez, J. L., Casas López, J. L., Plaza-
723 Bolaños, P., 2020. Neutral or acidic pH for the removal of contaminants of emerging concern in
724 wastewater by solar photo-Fenton? A techno-economic assessment of continuous raceway pond
725 reactors. *Sci. Total Environ.* 736, 139681. doi: 10.1016/j.scitotenv.2020.139681.

726 Scheierling, S. M., Bartone, C. R., Duncan Mara, D., Drechsel, P., 2011. Towards an agenda for
727 improving wastewater use in agriculture. *Water Int.* 36, 420-440. doi:
728 10.1080/02508060.2011.594527.

729 Schowanek, D., Feijtel T.C.J., Perkins C.M., Hartman F.A., Federle T.W., Larson R.J., 1997.
730 Biodegradation of [S,S], [R,R] and mixed stereoisomers of ethylene diamine disuccinic acid (EDDS),
731 a transition metal chelator, *Chemosphere* 34 (11), 2375–2391. doi: 10.1016/s0045-6535(97)00082-9.

732 Silhavy, T. J., Kahne, D., Walker, S., 2010. The bacterial cell envelope. *Cold Spring Harb Perspect*
733 *Biol.* 2, a000414. doi: 10.1101/cshperspect.a000414.

734 Silverman, A. I., Tay, N., Machairas, N. 2019. Comparison of biological weighting functions used to
735 model endogenous sunlight inactivation rates of MS2 coliphage. *Water Res.* 151, 439-446. doi:
736 10.1016/j.watres.2018.12.015.

737 Van Griecken, R., Marugán, J., Pablos, C., Furones, L., López, A., 2010. Comparison between the
738 photocatalytic inactivation of Gram-positive *E. Faecalis* and Gram-negative *E. coli* faecal
739 contamination indicator microorganisms. *Appl. Catal. B.* 100, 212-220. doi:
740 10.1016/j.apcatb.2010.07.034.

- 741 Villarín, M. C., Merel, S., 2020. Paradigm shifts and current challenges in wastewater management.
742 J. Hazard. Mater. 390, 122139. doi: 10.1016/j.jhazmat.2020.122139.
- 743 Voumard, M., Giannakis, S., Carratalà, A., Pulgarin, C., 2019. *E. coli* – MS2 bacteriophage
744 interactions during solar disinfection of wastewater and the subsequent post-irradiation period. Chem.
745 Eng. J. 359, 1224-1223. doi: 10.1016/j.cej.2018.11.055.
- 746 Wang, D., Hubacek, K., Shan, Y., Gerbens-Leenes, W., Liu, J., 2021. A Review of Water Stress and
747 Water Footprint Accounting. Water 13, 201, doi:10.3390/w13020201.
- 748 Wu, Y., Brigante, M., Dong, W., de Sainte-Claire, P., Mailhot, G., 2014. Toward a Better
749 Understanding of Fe(III)–EDDS Photochemistry: Theoretical Stability Calculation and Experimental
750 Investigation of 4-tert-Butylphenol Degradation. J. Phys. Chem. A 118, 396-403. doi:
751 10.1021/jp409043e.